AD-A137 317 NEW HIGH POWER COHERENT RADIATION SOURCES(U) NAVAL RESEARCH LAB WASHINGTON DC P SPRANGLE ET AL. 09 JAN 84 NRL-MR-5224 1/1

UNCLASSIFIED F/G 20/3 NL

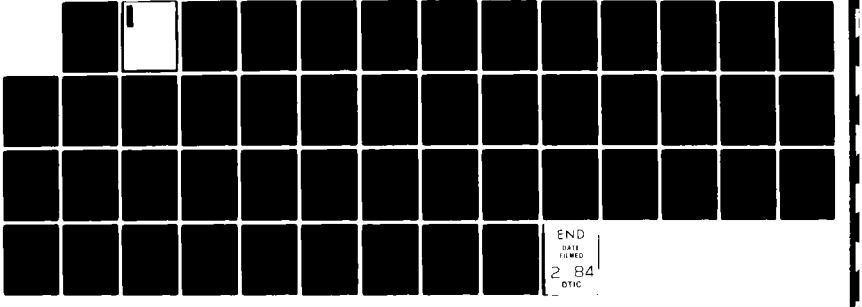

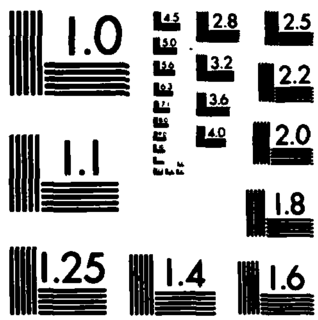

MICROCOPY RESOLUTION TEST CHART
NATIONAL BUREAU OF STANDARDS-1963-A

SECURITY CLASSIFICATION OF THIS PAGE (When Data Entered)

REPORT DOCUMENTATION PAGE	READ INSTRUCTIONS BEFORE COMPLETING FORM
1. REPORT NUMBER NRL Memorandum Report 5224 AD-A137317	2. GOVT ACCESSION NO. 3. RECIPIENT'S CATALOG NUMBER
4. TITLE (and Subtitle) NEW HIGH POWER COHERENT RADIATION SOURCES	5. TYPE OF REPORT & PERIOD COVERED Interim report on a continuing NRL problem. 6. PERFORMING ORG. REPORT NUMBER
7. AUTHOR(s) P. Sprangle and T. Coffey	8. CONTRACT OR GRANT NUMBER(s)
9. PERFORMING ORGANIZATION NAME AND ADDRESS Naval Research Laboratory Washington, DC 20375	10. PROGRAM ELEMENT, PROJECT, TASK AREA & WORK UNIT NUMBERS 61153N; RR011-09-4E; 47-0924-B-3
11. CONTROLLING OFFICE NAME AND ADDRESS Office of Naval Research Arlington, VA 22217	12. REPORT DATE January 9, 1984 13. NUMBER OF PAGES 47
14. MONITORING AGENCY NAME & ADDRESS(if different from Controlling Office)	15. SECURITY CLASS. (of this report) UNCLASSIFIED 15a. DECLASSIFICATION/DOWNGRADING SCHEDULE
16. DISTRIBUTION STATEMENT (of this Report) Approved for public release; distribution unlimited.	
17. DISTRIBUTION STATEMENT (of the abstract entered in Block 20, if different from Report)	
18. SUPPLEMENTARY NOTES	
19. KEY WORDS (Continue on reverse side if necessary and identify by block number) High power microwaves Relativistic electron beams	
20. ABSTRACT (Continue on reverse side if necessary and identify by block number) New coherent-radiation sources show considerable promise for producing power, at wavelengths from the millimeter to the ultraviolet regime, at previously unattainable levels and efficiencies. Some initial applications can already be identified.	

DD FORM 1 JAN 73 1473 EDITION OF 1 NOV 65 IS OBSOLETE
S/N 0102-014-6601

SECURITY CLASSIFICATION OF THIS PAGE (When Data Entered)

CONTENTS

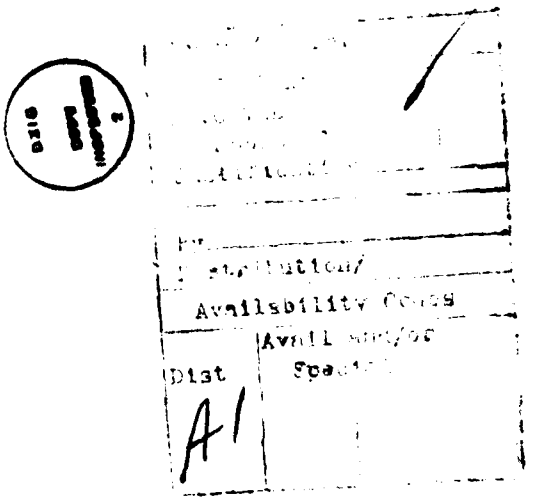

NEW HIGH POWER COHERENT RADIATION SOURCES

I. General Introduction

In recent years, there has been considerable renewed interest in the development of novel devices for the production of high power coherent electromagnetic radiation. This interest has been motivated largely by the realization that, with existing technology, certain processes utilizing relativistic electron beams can produce coherent electromagnetic radiation at power levels far in excess of those achieved by conventional electron devices. This paper will review the current status of this rapidly developing field, with emphasis on two generic devices.

The major thrust in the recent development of electron beam driven radiation sources has been directed towards achieving shorter wavelengths, greater power and higher efficiencies. Shortly after the development of such successful sources as the magnetron, klystron and various traveling wave devices, it became clear that, in their original form, they were limited in their ability to produce high levels of radiation efficiently at short wavelengths. To circumvent the inherent limitations of these conventional coherent radiation sources, many new concepts and mechanisms, as well as variations on conventional concepts, were proposed.

This paper is
~~We will be~~ concerned primarily with two devices which are, relatively speaking, newcomers to the list of coherent classical radiation sources. They are the free electron laser (FEL) and the cyclotron resonance maser (CRM); one well known type of CRM is the gyrotron. These sources have a great potential for extending the available range of wavelengths and power levels while maintaining high operating efficiencies. The potential merits of the FEL mechanism are numerous and include, among other things, high operating efficiencies (> 20%), tunability over a relatively broad frequency range and the ability to operate from the millimeter to the ultra

Manuscript approved October 17, 1983.

violet regime. The CRM mechanism offers high power capability at centimeter and millimeter wavelengths. Some of the areas of application for these sources are spectroscopy, advanced accelerators, short-wavelength radars, and plasma heating in fusion reactors.

The general purpose of this article is threefold: i) to briefly describe the physical mechanism of both the FEL and CRM, ii) to present an overview of the experimental programs pertaining to these sources, and iii) to discuss the present and future areas of application for these new sources.

The FEL and CRM are actually generic terms which apply to a wide class of coherent sources. These sources can operate either as amplifiers or oscillators over a wide range of wavelengths. The basic physical mechanisms on which these sources operate are fundamentally different. Although the basic process of exciting stimulated radiation is intrinsically quantum mechanical in nature, both the FEL and CRM can be adequately described by classical models.

Following the classical point of view, the origin of stimulated radiation from say, a system of electrons, is due to induced macroscopic currents. The induced macroscropic electron current, resulting from an imposed electromagnetic field, will,if properly phased, generate radiation which reinforces the original field. Since, in this basic amplification mechanism, the electron's kinetic energy is the source for the radiation, they must necessarily be initially streaming and/or gyrating. In an amplifier the imposed field is supplied from an external source whereas in an oscillator or superradiant amplifier the imposed field is internally generated, originating from single particle spontaneous radiation.

II. Free Electron Lasers

One of the first to propose the mechanism now referred to as the FEL concept was H. Motz. The first notable successful demonstration of this concept was realized in 1960 by Phillips. His device, which he called a Ubitron, employed a periodic magnetic field and operated as an amplifier in the millimeter regime. Although the basic mechanism of emission does not rely upon relativistic effects, one must use highly relativistic electrons to generate short wavelength radiation.

The FEL consists of three basic components: an electron beam, an external pump field and a radiation field[1-5]. Typically the pump field consists of a static periodic magnetic field. However, any field which induces a transverse electron oscillation could, in principle, function as a pump field; for example, a static periodic electric field or an electromagnetic field.

Unlike most conventional sources, the radiation wavelength in the FEL is not fixed or determined by the physical size of the containing structure. Short wavelength operation can therefore be achieved in rather large structures. Furthermore, since the lasing medium consists of a pump field, breakdown damage cannot occur in the interaction region. Hence, high power levels at short wavelengths can, in principle, be generated by this mechanism.

A. Physical Mechanism of the Free Electron Laser

In order to be specific in our discussions of the FEL mechanism we will consider only the more common type of pump field: a static periodic magnetic "wiggler." The primary field component of the magnetic wiggler is transverse to the main direction of flow of both the electron and radiation

beams, as shown in Fig. (1). As the injected electrons stream through the wiggler field they undergo coherent transverse oscillations due to the $\underset{\sim}{v} \times \underset{\sim}{B}$ force, hence the name wiggler. Since the oscillations are in the same direction as the radiation electric field the electrons can lose or gain energy. At the injection point the electrons are randomly phased and in the absence of a force to bunch them, they would radiate incoherently, generating spontaneous magnetic bremsstrahlung radiation. The essential feature of the FEL mechanism is that the electrons undergo axial bunching in the combined wiggler and radiation fields. It is the so-called "ponderomotive wave" produced by the beating of the wiggler and radiation field which results in electron bunching and hence the generation of coherent radiation (see e.g. the articles in ref. (5a) by F.A. Hopf et.al. N.M. Kroll et.al., A. Szöke et.al., P. Sprangle et.al. and W. B. Colson and S. K. Ride). The ponderomotive wave plays the same role as the slow traveling electromagnetic wave in conventional traveling wave sources (see e.g. P. L. Morton, ref. (5b)).

To better understand the origin and central role played by the ponderomotive wave, we will represent the wiggler magnetic field by $\underset{\sim}{B}_w = B_w \cos(k_w z)\hat{e}_y$ and the radiation electric and magnetic fields by $(\underset{\sim}{E}_R, \underset{\sim}{B}_R) = E_R \cos(kz - \omega t)(\hat{e}_x, \hat{e}_y)$. The radiation frequency, wavenumber and wavelength are assumed related by the vacuum relation, $\omega = ck = 2\pi c/\lambda$ and the wiggler wavenumber is $k_w = 2\pi/\lambda_w$ where λ_w is the wiggler period. Electrons streaming through these fields with axial velocity $v_o\hat{e}_z$ will (to lowest order) undergo forced transverse oscillations, see Fig. (1). This transverse velocity is referred to as the "wiggle" velocity and is given by $\underset{\sim}{v}_w = |e|B_w/(\gamma_o m_o c k_w) \sin(k_w z)\hat{e}_x$ where e is the electronic charge, $\gamma_o = (1 - v_o^2/c^2)^{-1/2}$ is the relativistic mass factor and m_o is the electron

beams, as shown in Fig. (1). As the injected electrons stream through the wiggler field they undergo coherent transverse oscillations due to the $\underset{\sim}{v} \times \underset{\sim}{B}$ force, hence the name wiggler. Since the oscillations are in the same direction as the radiation electric field the electrons can lose or gain energy. At the injection point the electrons are randomly phased and in the absence of a force to bunch them, they would radiate incoherently, generating spontaneous magnetic bremsstrahlung radiation. The essential feature of the FEL mechanism is that the electrons undergo axial bunching in the combined wiggler and radiation fields. It is the so-called "ponderomotive wave" produced by the beating of the wiggler and radiation field which results in electron bunching and hence the generation of coherent radiation (see e.g. the articles in ref. (5a) by F.A. Hopf et.al. N.M. Kroll et.al., A. Szöke et.al., P. Sprangle et.al. and W. B. Colson and S. K. Ride). The ponderomotive wave plays the same role as the slow traveling electromagnetic wave in conventional traveling wave sources (see e.g. P. L. Morton, ref. (5b)).

To better understand the origin and central role played by the ponderomotive wave, we will represent the wiggler magnetic field by $\underset{\sim}{B}_w = B_w \cos(k_w z)\hat{e}_y$ and the radiation electric and magnetic fields by $(\underset{\sim}{E}_R, \underset{\sim}{B}_R) = E_R \cos(kz - \omega t)(\hat{e}_x, \hat{e}_y)$. The radiation frequency, wavenumber and wavelength are assumed related by the vacuum relation, $\omega = ck = 2\pi c/\lambda$ and the wiggler wavenumber is $k_w = 2\pi/\lambda_w$ where λ_w is the wiggler period. Electrons streaming through these fields with axial velocity $v_o\hat{e}_z$ will (to lowest order) undergo forced transverse oscillations, see Fig. (1). This transverse velocity is referred to as the "wiggle" velocity and is given by $\underset{\sim}{v}_w = |e|B_w/(\gamma_o m_o c k_w) \sin(k_w z)\hat{e}_x$ where e is the electronic charge, $\gamma_o = (1 - v_o^2/c^2)^{-1/2}$ is the relativistic mass factor and m_o is the electron

rest mass. Typically, the electron wiggler velocity is much less than the axial electron velocity and much greater than the radiation induced transverse velocity. The force on the electrons responsible for longitudinal bunching is the ponderomotive force and originates from the $\underset{\sim}{v}_w \times \underset{\sim}{B}_R$ term in the electron force equation. The ponderomotive force, which in our illustration is proportional to $\sin((k + k_w)z - \omega t)\,\hat{e}_z$, is directed along the z-axis. The phase velocity of this longitudinal wave, also commonly referred to as the "trapping" or "bunching" wave, is $v_{ph} = \omega/(k + k_w)$ and is approximately matched to the electron axial velocity, i.e., $v_{ph} \approx v_o$. Synchronism between the ponderomotive wave and streaming electrons results in bunching and occurs when the radiation frequency equals $\omega = (1 - v_o/c)^{-1} v_o k_w$. For highly relativistic electron beams ($v_o \approx c$) the radiation wavelength, $\lambda \approx \lambda_w/2\gamma_o^2$, is substantially smaller than the wiggler wavelength and can be varied by changing the electron beam energy. Note that the wavelength associated with the ponderomotive wave and therefore with the bunched electron beam is very nearly equal to the radiation wavelength.

The process of electron bunching and energy extraction is illustrated in Fig. (2) for an injected beam of mono-energetic electrons. Electrons, with a sufficiently small energy spread, streaming with an axial velocity approximately equal to the ponderomotive wave velocity (actually slightly greater) are bunched in a continuous manner within the interaction region. In the presence of the wave, some electrons are decelerated while others are accelerated. Since initially the electron axial velocity is slightly greater than the wave phase velocity, those that are decelerated move closer to resonance while those that are accelerated get further from resonance. The average electron energy therefore is decreased. The

bunching of the decelerated electrons leads to an enhancement of the radiation field which in turn increases the electron density modulation and further increases the coherence of the growing radiation field.

The amount of energy spread on the electron beam is a crucial factor in the operation of the FEL especially at shorter wavelengths. Large beam energy spreads will substantially reduce the bunching and energy extraction process. The process of electron bunching and energy extraction in the wiggler region itself thermalizes the electrons and results in an increase of the beam energy spread. This effect places limits on the use of cyclic electron beams for FEL applications since electrons would repeatedly pass through the wiggler field and become thermalized.

For an alternative hybrid field configuration, a longitudinal magnetic field can be added [6,7], which, as we will describe, is one of the basic features of the cyclotron-resonance maser.

B. Free Electron Laser Operating Regimes

Existing accelerator technology together with the characteristics of the FEL interaction mechanism divide FEL's into distinct categories [2-5]. These categories are distinguished primarily by the type and characteristics of the electron beam source.

Free electron lasers based on such beams as RF linacs, microtrons or storage rings can be expected to operate in what is referred to as the "Compton" regime. Such beams are generally of high energy, low current and high quality (low emittance). The Compton regime is one in which the interaction physics is primarily governed by single-particle effects; collective or space charge effects can be neglected. Typically in this regime the radiation gain is low, thus, practical sources operating in this

regime would necessarily function as oscillators where high gain is not a crucial requirement. In the absense of efficiency enhancement techniques, the operating efficiencies are generally low, (e.g., a fraction of a percent). Since the beam energy and quality is generally high, FEL's in this regime can operate in the optical regime or beyond.

Free electron lasers based on intense relativistic electron beams (IREB) such as, Pulse line accelerators [8] or Induction Linac accelerators [9], operate in the "Raman" or "Collective" regime [2,4 and articles in 5a, e.g., D. B. McDermott and T. C. Marshall]. Here collective effects play an important role in determining such features as the radiation growth rate, interaction efficiency, etc. The FEL operating wavelength, however, remains well approximated by the expression appropriate for the Compton regime, i.e. $\lambda \approx \lambda_w/2\gamma_o^2$. Numerous FEL experiments have been performed with Pulse line generated beams. These beams are produced from plasma induced field emission diodes, and have a relatively flat voltage and current pulse lasting for a few tens of nanoseconds. Typically they are in the MeV energy range and carry kiloamperes of current. The low energy and quality of these beams limit their operation in FELs to the millimeter regime. Since the beam current is high, the radiation gain (or spatial growth rate) can be large enough to make operation as an FEL amplifier possible.

There is a third operating regime which has features that are common to both the Compton and Raman regimes. Here the wiggler field is strong enough so that the ponderomotive force on the electrons completely dominates the space charge forces and the radiation growth rate is large. We will refer to this regime as the "High-Gain Compton" [2,4].

The evolution of the radiation field is governed by the induced driving current which is of the form

$$\underset{\sim}{J}_{\perp} = - |e| F\delta n \underset{\sim}{v}_{w},$$

where δn is the electron density perturbation resulting from the bunching effect of the ponderomotive wave and space charge wave potential, $\phi_{pond} = |e| B_w E_R (2k_w k \gamma_o m_o c^2)^{-1} \cos((k + k_w)z - \omega t)$ is the ponderomotive wave potential and ϕ_{sc} is the space charge wave potential due to collective effects and F is a filling factor which takes into account the fact that the radiation and electron beam do not in general completely overlap (F = electron beam area/radiation beam area). The phase of the induced current, which is proportional to the radiation through δn, is such that it reinforces the radiation field.

The radiation gain, or growth rates, are found by solving the wave equation with the induced driving current together with collective effects. Table I list the various expressions for the gain, or spatial growth rates, and the corresponding intrinsic energy efficiencies for the FEL operating regimes [4, 10]. The intrinsic power efficiencies were obtained from nonlinear calculations of electron trapping in the ponderomotive wave. Later various methods will be discussed which can dramatically increase these values. The expressions in Table I were obtained for mono-energetic beams having no initial energy spread. However, if the fractional beam energy spread is much less than the value of intrinsic efficiency the beam can in fact be considered mono-energetic. In the Compton regime the radiation gain per pass and intrinsic efficiencies are usually low, values of 0.1 and 1% respectively are typical. In fact, in this regime, the intrinsic efficiency as given in

Table I

The quantities used in Table I have the following definitions $\nu = I/17$ is Budker's parameter, I is the beam current in kilo amperes, L is the wiggler length, r_b is the beam radius, $\beta_w = v_w/c$, $\gamma_z = \gamma/(1 + \gamma^2\beta_w^2)^{1/2}$, $f(\theta) = \partial\ (\sin\theta/\theta)^2/\partial\theta$, $\theta = (1 - v_o/v_{ph})\tau\omega/2$ and $\tau = L/v_o$ is the electron's transit time. (c.g.s. units are used unless otherwise stated)

FEL Operating Regimes	Gain or Growth Rate	Intrinsic Power Efficiency
Compton (single-particle, low-gain)	$\pi F \frac{\nu}{\gamma} (\beta_w)^2 \frac{L^3}{r_b^2 \lambda_w} f(\theta)$	$\frac{1}{2} \frac{\lambda_w}{L}$
Raman (collective, high gain)	$(\pi\gamma_z F)^{1/2} (\nu/\gamma)^{1/4} \frac{\beta_w}{\sqrt{r_b \lambda_w}}$	$\frac{1}{\pi\gamma_z} (\frac{\nu}{\gamma})^{1/2} \frac{\lambda_w}{r_b}$
High Gain-Compton (single-particle)	$2 F^{1/3} (\frac{\nu}{\gamma})^{1/3} (\frac{r_b}{\lambda_w})^{1/3} \frac{\beta_w^{2/3}}{r_b}$	$0.18 (\frac{\nu}{\gamma})^{1/3} (\frac{\lambda_w \beta_w}{r_b})^{2/3}$

Table I is $\lambda_w/(2L)$, which is just the inverse of twice the number of wiggler periods in the interaction length. In the next section we will see that these low efficiencies can be dramatically increased to as much as 20%. The condition to neglect space charge forces on the trapped electrons, in the Compton regime, is that the ponderomotive potential be much greater than the space charge potential, i.e., $|\phi_{pond}| >> |\phi_{sc}|$. This condition can be stated as a limitation on the electron beam density, $n << \gamma B_w E_R/(4\pi m_o c^2)$. In the Raman regime the radiation growth rates and efficiencies can be very high, e-folding lengths of a few centimeters and intrinsic efficiencies as high as 15% are possible.

C. Enhancement of Wave-Particle Interaction Efficiency

One of the most potentially attractive features of the FEL (besides its high power capability and frequency tunability) is the impressively high efficiency of converting electron beam power to radiation power. Higher operating efficiencies can be achieved by either improving the efficiency of the wave-particle interaction process or by recovering a portion of the electron kinetic energy after they have taken part in the interaction.

Improvements in the wave-particle interaction efficiency can be made by decreasing the phase velocity of the ponderomotive wave while the electrons are trapped within the wave, and/or applying a longitudinal accelerating force to the trapped electrons[5a,10]. To visualize the underlining physics in the first approach we recall that during the initial stage of the FEL interaction the electrons become trapped in the ponderomotive wave and lose a small amount of kinetic energy which is

converted to radiation energy. If the process is allowed to continue the trapped electrons will undergo slow longitudinal synchrotron oscillations in the trapping wave and periodically exchange energy with the radiation field until they become thermalized. The potential wells associated with the trapping wave are referred to as trapping "buckets". If, as the wave and trapped electrons travel through the interaction region, the phase velocity of the wave is gradually decreased as a function of axial distance, substantially more kinetic energy can be removed from the electrons. If the decrease in phase velocity is sufficiently gradual the electrons will remain trapped and the radiation field and hence efficiency will increase dramatically. This can be accomplished in a straightforward way by recalling that the phase velocity of the trapping wave is $v_{ph} = \omega/(k + k_w) \approx c(1 - \lambda/\lambda_w)$. Hence, by spatially decreasing the wavelength of the wiggler field, the phase velocity of the wave can be decreased resulting in enhanced efficiency.

In the second approach, which can be employed in conjunction with the first, a longitudinal accelerating force is applied to the trapped electrons. Since the electrons are trapped, this force does not lead to acceleration but results in a relative phase shift of the electrons in the trapping buckets. The phase shift is such that the electrons perform work on the trapping wave resulting in radiation growth. The accelerating force may take the form of an external uniform axial electric field. Another, perhaps more practical approach, is to spatially decrease the amplitude of the wiggler field. To see this, we will neglect for the moment the presence of the radiation field, and note that if the wiggler field amplitude is decreased, the electron transverse velocity decreases and the axial velocity increases (total electron energy is conserved). However, if

the radiation field is present and the electrons are trapped, decreasing the wiggler field simply results in the electrons performing work on the trapping wave without a change in their axial velocity. Enhanced growth of the radiation field can therefore be achieved by either decreasing the wiggler period and/or amplitude. These schemes can be applied to either the Compton or Raman operating regimes of the FEL. In the trapped particle mode of operation of the FEL, N. M. Kroll and M. N. Rosenbluth found that it is possible for the trapped electrons to become unstable resulting in sideband radiation [5a].

D. Enhancing Efficiency by Recovering Beam Energy

Another FEL efficiency enhancement approach involves recovering or reusing the electron beam kinetic energy after it has passed through the interaction region [see e.g. L. R. Elias and G. Ramian, ref. 5c]. The particular method used to recover the energy in the spent electrons depends upon the type of electron source employed. With D.C. electrostatic accelerators, such as Van de Graffs, energy recovery can be achieved by reversing the acceleration process on the spent electrons with a voltage depressed collector. This method is called "D.C. energy recovery" and is a commonly employed efficiency enhancement technique in conventional microwave tubes.

For FELs employing RF linacs or microtron accelerators, an "RF energy recovery" approach can be used. Such accelerators generate beams which consist of periodically spaced micro pulses which upon emerging from the FEL interaction region can be decelerated in an RF structure and their kinetic energy efficiently converted back into RF energy.

E. Overview of Free Electron Laser Experimental Programs

To date, a relatively small number of experimental studies of the FEL have been performed (although numerous experiments throughout the world are either underway or in the planning stage). These experiments have been directed at verifying the many phenomena predicted by theory. In this sense the early experiments have been successful, indicating that the FEL may indeed become a practical, tunable source of radiation. Many of the experiments now underway or in the planning phase will employ efficiency enhancement techniques and attempt to extend the operating range into the visible regime and beyond.

Pioneering FEL experiments in the Compton regime have been performed by the Stanford University group [11,12] using the Stanford Superconducting Linear Accelerator (SCA), see table IIa. These experiments were primarily designed to verify some of the important theoretical predictions such as gain per pass, efficiency, etc.

The Stanford group's most recent FEL oscillator experiment, headed by J. Madey, [12] is illustrated schematically in Fig (3). The pump field consisted of a 2.3 kG helical magnetic wiggler having a 3.3 cm wavelength and overall length of 5.3 m. The 43 MeV electron beam from the SCA consisted of a series of micro electron beam pulses 1.0 mm in length with a pulse spacing of approximately 25.4 m. The peak micro pulse current was approximately 1.3 A and the macro beam pulse (series of micro pulses) lasted for 1.5 msec. The fractional energy spread of the SCA electron beam is on the order of 5×10^{-4}. Spontaneous radiation from the individual electrons, within the wiggler region, occurred at a central wavelength of 3.3 μm and had a line width equal to $\Delta\lambda/\lambda \approx 0.01$. The build up of incoherent radiation into intense coherent radiation occurred because the

Table IIa

FEL Experiments Employing RF Linacs and Microtrons

Laboratory	Class	Wave-Length (μm)	Beam Energy (MeV)	Peak Current (A)
Stanford U.	A	10.6	24	0.1
Stanford U.	O	10.6	43	1.3
MSNW/Boeing	A	10.6	20	0.2
LASL	A	10.6	20	10
LASL	O	10.6	20	30-60
TRW	A	10.6	25	10
NRL	O	16.0	35	5
Bell Lab*	A	100-400	10-20	5
Frascati*	A	16	20	0.6
TRW/Stanford	O	1.6	66	0.5-2.5

A: amplifier O: oscillator

*Microtron beam source

gain spectrum associated with the FEL process was also peaked at around 3.3 μm. The separation of the optical resonator mirrors was carefully adjusted so that the round trip bounce time of the radiation pulses just equaled the time interval between electron micro pulses. In the experiment the mirror separation was approximately 12.7 m, approximately half the separation between the micro beam pulses. This insured that the entering electron pulses were in approximate synchronism with the radiation pulses. For illustrative purposes, Fig. (3) shows multiple beam pulses within the resonator, the Stanford experiments however were designed so that a single pulse was within the resonator at any given instant. Due to a small but important effect called laser "lethargy" the radiation pulses traveling with the electron pulses will have a velocity slightly less than the electron pulse velocity [e.g. F. Hopf et al. in 5a and W. Colson in 5b]. The radiation pulses, therefore, tend to fall behind the electron pulses. To overcome this lethargy effect the mirror separation must be slightly less than would be expected if the radiation pulses traveled at the velocity of light. Under conditions of synchronism the intensity of the radiation pulses build up in the cavity with successive incoming beam pulses. The measured peak output power was 6kW and since the round trip mirror losses were 1.5%, the peak radiation power within the resonator was 400 kW. The measured linewidth of the saturated radiation was $\Delta\lambda/\lambda \approx 6 \times 10^{-3}$ and the 6% measured gain per pass was in fair agreement with the theoretical value of ~10%.

At Los Alamos an experimental program is underway to develop a highly efficient FEL oscillator source [12,13]. The FEL will employ an RF linac accelerator and radiate at 10.6 μm. To enhance efficiency in the Los Alamos experiment the wiggler wavelength and amplitude will be spatially

varied and RF energy recovery methods employed. A 20% overall efficiency is anticipated, this should result in an average output power of 100 kW. The FEL oscillator in this experiment is expected to saturate because of electron trapping. In the trapped particle mode of operation, numerical simulations [14,15] show that sideband frequencies can grow and lead to chaotic behavior thus reducing the quality of the radiation pulse. However, by introducing frequency filters and/or by increasing the cavity losses, these sideband frequencies can be controlled. Preliminary experimental measurements are in excellent agreement with theory and show deceleration of trapped electrons by as much as 7% and extraction of more than 3% of the total beam energy when the FEL is operated as an amplifier.

A joint MSNW/Boeing Aircraft experiment is directed towards developing an optical (0.5 μm) FEL oscillator employing an RF linac beam with a peak current of 100A [12,13].

At the Naval Research Laboratory a recent FEL experiment [13] using an IREB has produced 35 MW of power at a wavelength of 4 mm (see table IIc). The low energy spread of the injected pulse line generated electron beam was a particularly novel feature of this experiment. The FEL in this experiment operated as a superradiant amplifier with an interaction efficiency of 2.5%. Experimental FEL programs employing high current pulse line generated beams are also being performed at Columbia Univ. [5a] and MIT [5c] among other places.

Experiments at Santa Barbara are presently underway to evaluate the D.C. beam recovery scheme using a 6 MeV Van de Graff accelerator, table IIb. The FEL is designed to operate at 200 μm and achieve an output power of 12 kW.

Two induction linac FEL experiments are underway in the United States,

Table IIb

FEL Experiments Employing Electrostatic and Induction Linac Accelerators

Laboratory	Accelerator	Wave-length (mm)	Beam Energy (MeV)	Peak Current (A)
UCSB	Electro-Static Accel.	0.1-1	6	2
UCSB	Electro-Static Accel.	0.36	3	2
NRL	Induction Linac	8	0.7	200
LLNL	Induction Linac	3-8	4	400

Table IIc

FEL Experiments Employing Pulse Line Generated Beams*

Laboratory	Peak Power (MW)	Wave-length (mm)	Beam Energy (MeV)	Beam Current (kA)
NRL	1	0.4	2	30
Columbia U.	8	1.5	0.86	5
Columbia U.	1	0.6	0.9	10
NRL/ Columbia U.	1	0.4	1.2	25
NRL	35	4	1.35	1.5
MIT	1.5	3	1	5
Ecole Poly	2	2	1	2

* Typical pulse times are tens of nanoseconds.

one at NRL and the other at LLNL. These experiments, see Table IIb, will operate in the Raman regime. In the LLNL experiments, headed by A. Sessler and D. Prosnitz, the FEL is operated as an amplifier since the 5 MeV induction linac beam (ETA) has a pulse length of ~ 50 nsec [5c,12]. The induction linac FEL experiments at NRL headed by C. Kapetanakos and J. Pasour, has a uniquely long pulse duration (about 2 μ sec); hence, the FEL source can therefore operate as an oscillator [16]. Presently it is operated as a superradiant amplifier, generating 4.2 MW at a wavelength of 8 mm and efficiency of 3%.

A number of FEL experiments using electron storage rings are in progress, (see table IId). In a storage ring FEL the electrons interact with the wiggler, located in one of the straight sections, during each revolution. Since the electrons may undergo several billion revolutions, competition between electron thermalization in the FEL region and electron cooling due to synchrotron radiation, will limit the output laser power to a small fraction of the total synchrotron radiation emitted, thus limiting the FEL efficiency to around 1 % or less, (see e.g., C. Pellegrini, ref. (5a)). The National Synchroton Light Source Storage Ring facility at Brookhaven National Laboratory is scheduled to be used for FEL experiments this year. In these studies the storage ring will operate at 500 MeV at a peak current of 108A. It is expected that the radiation gain will be around a few per cent and at a wavelength of about 3500 Å.

F. Future Direction of Free Electron Laser Research

Since wiggler wavelengths are limited to a few centimeters, optical FELs require electron beam energies of ~ 50 MeV or greater. To overcome the need for such high energies, a high frequency electromagnetic pump

Table IId

FEL Experiments Employing Storage Ring Beams

Laboratory	Storage Ring	Wave-Length (μm)	Beam Energy (MeV)	Beam Current (A)	measured gain/pass (%)
Orsay	ACO	0.5	240	2 (peak) 0.03 (ave.)	0.07
Frascati	ADONE	0.5	600	10 (peak) 0.1 (ave.)	0.02
Novosibirsk	VEPP-3	6	340	20(peak)	0.4
BNL	VUV (underway)	0.35	500	108 (peak) 1.0 (ave)	2.0 calculated
Stanford U.	ARRL (planned)	0.5	1000	200 (peak) 1.0 (ave.)	-

field, such as an intense laser beam or the output of another FEL source, could be used. Using a powerful CO_2 laser pump propagating anti-parallel to the electron beam, the Doppler shifted FEL radiation wavelength becomes $\lambda \approx \lambda_L/4\gamma_o^2$ where λ_L is the laser pump wavelength. For a CO_2 laser pump, a 1 MeV electron beam the FEL could in principle produce radiation in the optical regime. Another interesting alternative is a two stage FEL scheme in which a single electron beam is used. Here the first stage is basically identical to the usual FEL using a wiggler field. The radiation produced in the first stage is reflected and becomes the pump field for the second stage. The final radiation wavelength is $\lambda \approx \lambda_w/8\gamma_o^4$. Therefore, electron beam energies of ~ 5 MeV would be necessary to obtain radiation in the optical regime. Both these schemes however can be shown to have a low gain per pass and since beams with extremely low energy spreads are necessary, the trapping efficiency is small. Efficiency enhancements schemes are limited to the accelerating electric field approach which was discussed earlier.

In 1984 the ATA electron beam at LLNL is scheduled to be used in FEL amplifier experiments. The expected 500 GW electron beam pulses could easily produce tunable multi gigawatt radiation pulses in the near optical regime.

The possibility of reversing the FEL process to achieve particle acceleration has been considered by a number of researchers [17]. The inverse FEL electron accelerator would employ an intense laser beam, e.g., CO_2, together with a wiggler to produce a large amplitude pondermotive wave which would trap and accelerate electrons. The trapped electrons could be energized by either increasing the period and/or amplitude of the wiggler field. The effective accelerating gradient is typically a few percent of

the laser electric field making accelerating gradients > 100 MeV/m possible. The diffraction properties of the laser beam, however, limit the acceleration length so that electrons gain at most a few GeV in a single stage. A major problem area associated with the FEL accelerator is the refocusing of the laser beam to achieve multi stage acceleration.

Charles Roberson et al. [5c] suggest that electron-beam sources for free-electron lasers could be intense cyclic electrons beams generated by race track induction accelerators or modified betatrons. These beams, however, are still in a proof-of principle development stage.

III. Cyclotron Resonance Maser

Cyclotron resonance masers [18-20], have reached a far more mature stage of development than FEL sources. Radiation sources based on the CRM mechanism are among the most efficient means for generating coherent high power radiation in the centimeter and millimeter wavelength regime. Devices based on the CRM mechanism, either oscillators or amplifiers, are commonly referred to as gyrotrons. The CRM mechanism appears to have been proposed independently by a number of researchers (R. Q. Twiss, J. Schneider, A. V. Gapanov and R. H. Pantell) in the late 1950's. These early theoretical studies demonstrated that relativistic effects associated with mono-energetic electrons in a magnetic field could dominate the absorption process and result in stimulated cyclotron emission. The first clearly defined experimental confirmation of the CRM mechanism was reported by Hirschfield and Wachtel in 1964.

The radiation wavelength in the CRM is primarily determined by the applied magnetic field. Although in CRM oscillators the cavity dimensions are determined by the operating wavelength, cavities with dimensions large

compared to a wavelength (overmoded cavities) can be employed. Hence, quite high power handling capabilities are possible with oscillators. The development of this concept into a practical radiation source took place in the USSR during the 1960's and 1970's [e.g., V. Flyagin et al. in 20] primarily at Gorkii State University. In the 1970's major advances were also made in the United States primarily at the Naval Research Laboratory as well as at MIT, Yale University, Varian and Hughes. The demonstrated efficiencies and power levels of the CRM in the millimeter regime are impressive. The Gorkii group, for example, as early as 1975 developed a 22 kW, CW oscillator source operating at λ = 2mm with a 22% efficiency.

A. Physical Mechanism of the Cyclotron Resonance Maser

In its simplest form the CRM consists of a beam of nearly mono-energetic electrons streaming along and gyrating about an external magnetic field $B_o \hat{e}_z$ as depicted in Fig. (4). The introduction of an electromagnetic field, primarily polarized in the transverse direction, can alter the particle orbits, producing phase bunching which reinforces the imposed radiation field [18]. To illustrate this physical process in its simplest terms the imposed field is assumed to have the form $\underset{\sim}{E} = E_o \cos \omega t \hat{e}_y$. This form closely approximates the transverse electric (TE) mode of a cavity or waveguide when ω is near one of the cut-off frequencies of the structure. The electrons behave as individual oscillators gyrating about the magnetic field, B_o, with a rotation frequency Ω_R given by the relativistic electron cyclotron frequency, $\Omega_R = \Omega_o/\gamma$ where $\Omega_o = |e|B_o/m_o c$, $\gamma = (1 - \beta_\perp^2)^{-1/2}$ is the relativistic mass factor and $v_\perp = c\beta_\perp$ is the transverse electron rotation velocity. The electron rotation frequency Ω_R is a function of the electron energy (nonisochronous

rotation). Since our model is independent of transverse coordinates, we may for the purpose of this discussion superimpose all the electrons onto a single cyclotron orbit. For the sake of simplicity we will consider the trajectories of only 8 electrons. Initially the electrons are uniformly distributed and rotate about the circular orbit shown in Fig (4a). With the initial polarization for the radiation field as shown, those particles in the upper half plane ($x>0$) will lose energy and therefore increase their rotation frequency. Those in the lower half plane will gain energy and hence decrease their rotation frequency. The variation in the electron's rotation frequency results in phase bunching. If the wave frequency is slightly greater than the average electron rotation frequency, i.e., $\omega \gtrsim \Omega_R$, the phase of the bunches will be such that the imposed radiation is amplified. A snapshot of the electron distribution after many periods of the radiation field ($2\pi/\omega$) shows that electrons become bunched in phase with the radiation field, see Fig. (4b). After an integer number of wave periods there will be more particles in the upper half plane than are in the lower half plane. Since those electrons in the upper half plane lose energy to the field, the field is reinforced (amplified). The physical picture presented here is insensitive to the initial phase chosen for the radiation field. Indeed the wave growth mechanism depends only on the fact that $\omega \gtrsim \Omega_R$, Ω_R is energy dependent and that all the particles have roughly the same transverse velocity. The CRM mechanism is similar to the well-known "negative mass" instability encountered in cyclic beams.

With this physical picture in mind we now describe briefly the overall operation of the CRM oscillator as shown in Fig. (5). Electrons, depending on their initial phase upon entering the cavity, will either gain or lose kinetic energy as discussed earlier. Those electrons that gain energy move

further from resonance with the cavity field while those that lose energy get closer to resonance with the field and lose energy faster. Thus, a net decrease in electron kinetic energy occurs within the cavity. If the electrons were to remain within the cavity they would eventually gain back a portion of their lost kinetic energy. However, in designing a CRM oscillator the cavity length is chosen such that the electrons exit the cavity when their average energy is minimum. Another important consideration for steady state operation of the oscillator is choosing the cavity's Q such that the radiated power just balances the rate of kinetic energy lost by the electrons.

The primary source of radiation energy in the CRM is the gyrational electron energy. For high efficiency operation it is, therefore, necessary that the ratio of transverse to longitudinal electron velocity, i.e., $v_\perp/v_z$, be large; typically this ratio is between 1 and 3. The efficiency of the CRM is the ratio of the decrease in average electron kinetic energy, upon exiting the cavity, to the input electron kinetic energy. It is given by $\eta = \eta_\perp/(1 - (v_z/v_\perp)^2)$ where $\eta_\perp$ is the "transverse efficiency" associated with the gyrational electron energy loss. Calculated values of transverse efficiences can be as high as 60%. Demonstrated efficiencies, which will be discussed shortly, can approach the calculated values.

The energy gained by the average, slightly relativistic, electron in traversing the CRM cavity is given by

$$\Delta W = \frac{(|e| E_o \tau)^2}{2m_o} \left[\frac{Q_R^2 \beta_\perp^2 \tau}{4} \frac{d}{d\Gamma} \left(\frac{\sin \Gamma}{\Gamma}\right)^2 + \left(\frac{\sin \Gamma}{\Gamma}\right)^2\right] \qquad (2)$$

where $\Gamma = (\omega - \Omega_R)\tau/2$ and τ is the electron transit time through the cavity. The two terms within the brackets in Eq. (2) form the cyclotron resonance absorption function which is plotted in Fig. (7). The first term in brackets is a relativistic contribution and can be negative resulting in an average decrease of electron energy and thus wave amplification. The second term is always positive and represents absorption of wave energy. A number of physical points, previously discussed, are reflected in Fig. (6). Maximuim wave amplification requires $\omega \gtrsim \Omega_R$ and occurs at $\Gamma \approx \pi/2$, lengthing the cavity (increasing τ) beyond this point leads to a decrease in wave amplification.

B. Efficiency Enhancement in Cyclotron Resonance Masers

There are basically two approaches that have been employed to enhance efficiency in CRMs above the intrinsic values. Both of these techniques rely on modifying the non-linear electron dynamics by spatially contouring various field profiles. In the first approach the longitudinal profile of the cavity radiation field is contoured by appropriately varying the cavity wall radius [20] as illustrated in Fig. (7). Electrons entering the cavity become phase bunched in a region where the field amplitude is small. In this region of the cavity, little energy extraction takes place. As the electrons travel through the cavity they enter the high field region, highly bunched. Energy extraction takes place in this region of the cavity and since the electrons have attained a higher degree of bunching than would otherwise be the case, the conversion efficiency is somewhat higher. The longitudinal profile of the electric field depicted in Fig. (7b) results from the fact that the operating frequency is chosen to be below cut-off near the entrance (small radius) and near cut-off at the exit

end of the cavity (large radius).

An alternative efficiency enhancement approach is to axially contour the external longitudinal magnetic field [21]. As the electrons traverse the cavity and lose energy it might appear at first glance, that to maintain the resonance condition, i.e. $\omega \gtrsim \Omega_0/\gamma$, the magnetic field should be spatially decreased. However, at high conversion efficiencies, non-linear effects dominate the wave-particle dynamics making small-signal considerations invalid. In fact, enhanced efficiency can be achieved by appropriately increasing the magnetic field. The mechanism at work here is similar in many respects to that in the first approach. The magnetic field near the input is made smaller than normally required allowing the electrons to phase bunch without losing or gaining much energy. As the degree of bunching increases the electrons find themselves in a higher magnetic field and are thus closer to resonance. Energy extraction takes place as the electrons are brought closer to resonance by increasing the magnetic field, see Fig. (7).

As with conventional microwave tubes and certain types of FELs the energy in the spent electrons can be recovered to a large degree by passing the spent electron beam into a voltage depressed collector, D.C. energy recovery. This technique can recover approximately 90% of the longitudinal energy in the used beam.

C. Development of Cyclotron Resonance Maser Sources

Magnetron injection guns are commonly used to produce the necessary electron beams for CRM sources. These thermionic, cross-field electron guns are capable of generating beams of several amperes of current and energies as high as 100 keV. Although 100 keV electrons are not generally

considered relativistic, these energies are perfectly satisfactory for CRM operation.

For millimeter wavelength radiation, the magnetic field is usually produced from superconducting sources. At the fundamental cyclotron harmonic a 34 kG magnetic field is required for the generation of 94 GHz (λ = 3 mm) radiation. For millimeter wave generation the magnetic field limitation of superconducting sources can be overcome by operating at higher cyclotron harmonics. The necessary magnetic field is thus reduced by approximately the harmonic number. The efficiency at the second harmonic remains high, in fact some designs show the efficiency at the second harmonic can be higher than at the fundamental. Generally, however, the efficiency falls sharply for operation beyond the second harmonic.

The radiation power handling capabilities of the CRM roughly scale directly with the cross sectional area of the electron beam and cavity size. Therefore, to increase the interaction volume for high power operation, highly overmoded cavities are used. These cavities operate in the TE mode and generally have low Qs. As an example of the state-of-the-art in high power devices, Soviet scientists [22] have produced 1.25 MW at 45 GHz (6.7 mm) with a pulse duration of 1-5 msec and 1.1 MW at 100 GHz (3.0 mm) with a pulse duration of 100 μsec. Both of these oscillator devices operated at the fundamental cyclotron harmonic with efficiencies of 34%. Another very impressive accomplishment of the Gorkii group is a 120 kW CRM operating at 375 GHz (λ = 0.8 mm) with pulse durations of 0.1 msec [23]. Recently in the U.S.A., Richard Temkin and his co-workers at MIT have achieved impressive power levels exceeding 180 kWs at 140 GHz.

High power millimeter wave CRMs will necessarily operate in a highly overmoded cavity in order to avoid excessive thermal loading and mode

competition problems. Recent results at the Naval Research Laboratory [24] have shown that highly overmoded CRMs can be stabilized by adding a small prebunching cavity in front of the large energy extraction cavity.

Prospects for the CRM amplifier to reach a practical stage of development are high. For example, researchers at the Naval Research Laboratory [19,25] have achieved impressive gains (18-56 dB) together with large useful bandwidths (2 - 13%) at 35 GHz at a typical power of 10 kW and an efficiency of 8%. Table III highlights the experimental oscillator and amplifier CRM program in the United States.

To extend the operating power and frequency of CRMs it has been suggested that the cavity be replaced with an open resonator[26]. This new configuration termed a "Quasi-Optical" CRM offers many potentially attractive features, among them are: very high frequency operation (submillimeter), mode selection and extremely high power handling capability. Preliminary experiments on this novel CRM configuration by the Yale University group are encouraging [27].

IV. Other Novel Sources

A number of other concepts for producing high power radiation have been suggested, which although at a very early stage of development, are worth noting. Among these concepts is the non-isochronic reflecting electron system, NIRES for short. Since the beam current in the NIRES is high, the self fields prevent the beam from propagating down a drift tube. Instead a "virtual cathode" is formed near the actual cathode-anode gap and the emitted electrons undergo oscillations between the actual and virtual cathode through the anode which consists of a thin metal foil. The oscillating electrons phase bunch, resulting in the generation of copious

Table IIIa

U.S. Experimental CRM Oscillators

Laboratory	Freq. (GHz)	Power (kw)	Eff (%)	Pulse Duration
Varian	28	340	45	Continuous
Varian	60	120	38	Continuous
NRL	35	340	54	1 μsec
MIT	140	180	30	1 μsec
Hughes	60	240	30	100 msec

Table IIIb

U.S. Experimental CRM Amplifiers

Laboratory	Freq. (GHz)	Power (kw)	Eff (%)	Pulse Duration	Bandwidth (%)
NRL	35	10	8	1.5 μsec	2-13%
Varian	28	65	9	1 msec	1
Varian	5	120	26	50 μsec	5
Yale U.	6	20	10	1 μsec	11

levels of radiation. Initial studies of this concept, which has the advantage of being compact, tunable and simple, have produced over 100 MWs of 3 cm radiation [28].

Coherent Cherenkov radiation is a less novel, but nonetheless an interesting millimeter source. Experiments in which a relativistic electron beam is propagated along a dielectric surface, have resulted in efficiencies of 10% and power levels of 100 kW at a wavelength of 4 mm [J. Walsh, ref. 5a].

In recent years a novel type of relativistic magnetron has come into existence which is capable of generating unprecedented levels of coherent radiation in the centimeter wavelength range. Using pulse line generated electron beam power levels as high as 10 GW have been reported [29].

V. Potential Applications

The free electron laser and the cyclotron resonance maser are sources with novel properties. The importance of these devices will, however, be ultimately determined by their utility, rather than their novelty. Nevertheless, there are a number of very interesting potential applications. Among these are applications to spectroscopy, accelerators, plasma heating and radars.

The application of the free electron laser to spectroscopy has recently been addressed by the National Academy of Sciences [30]. This study concluded that the FEL was a promising source for spectroscopic studies in wavelength regions $\lambda > 25$ μm and $\lambda < 200$ nm. The most attractive features of the FEL for spectroscopic applications are tunability, high average power, stable output power and frequency, short pulses with high peak powers, coherence and narrow bandwidth. These

features are especially important in the areas of condensed matter physics, spectroscopy of atoms, molecules, and ions, and surface studies in the presence of absorbed molecular species. The National Academy study points out that the short time duration (10^{-10} to 10^{-11} sec), available from some FEL sources, has important applications in the far infrared. These applications include the dynamics of charge carriers in semi-conductors, the dynamics of phonons, plasmons, and super-conducting gaps. Such studies are beyond the reach of any of the currently available sources in the 25 μm to 1000 μm region. The National Academy study points out that studies of vibrational relaxtion multi-photon processes, fast chemical kinetics, and photochemistry would be substantially strengthened by tunable picosecond pulses at high power for wavelengths less than 200 nanometers. The study also identifies a number of potentially important applications in surface chemistry. These include vibrational spectroscopy of absorbed molecules on single crystals, time resolved spectroscopy of the transient response of surface species, far infrared spectroscopy of metal oxide interfaces, and vibrational excitation of molecules reacting on a surface. The National Academy study emphasizes the point that the greatest benefit is likely to occur in the area of non-linear spectroscopy and in the area of transient studies.

High power microwave tubes have traditionally played a very important role in the development of RF accelerators. Future advances in high energy accelerator development will undoubtedly be closely tied to the economics of constructing new RF devices. It is possible that the development of very high power centimeter wave sources could be of considerable importance to the high energy accelerator community [17]. Conventional RF accelerators utilize microwave klystrons operating in the vicinity of 25

MWs of peak power. Recent developments indicate that FELs and CRMs operating at hundreds of megawatts or even gigawatt power levels are possible. These higher powers would translate into fewer power tubes, and therefore possibly lower total cost. The use of centimeter waves could lead to higher average accelerating gradients and therefore shorter accelerators. There are, of course, a number of practical and scientific questions which would have to be resolved prior to developing RF accelerators with FELs or CRMs as power sources. It must be demonstrated that the new power sources could deliver the required average power with acceptable efficiency. It would have to be demonstrated that stable acceleration could be achieved at the shorter wave lengths. Nevertheless, considering the potential benefit to high energy physics, it would appear that a research program aimed at the application of these new high power sources would be a prudent investment.

The problem of plasma heating is still a significant impediment to the practical development of magnetic fusion power reactors. The development of practical high power sources at millimeter wavelengths can have important applications to this problem. Recent experiments on the Oak Ridge ISXB Tokamak using a CRM developed at the Naval Research Laboratory, operating at 35 GHz demonstrated large absorption through the electron cyclotron resonance [19]. The absorption was accompanied by significant electron heating. Because of the low plasma density, ion heating was not expected and was not observed. However, as reactor conditions are approached with their higher densities and longer confinement times, these recent experimental results bode well for the application of high power CRMs to the heating of fusion plasmas. Free electron lasers are expected to be less efficient than CRMs for the production of millimeter waves,

hence, it is likely that CRMs will be more suitable for plasma heating than will FELs.

Most radar applications to date have been at microwave frequencies (i.e., centimeter waves and greater). This has been due primarily to the availability of power tubes and components and to the low atmospheric losses at these wavelengths. Since the FEL and CRM will lead to the development of sources in the millimeter wave region applications to radar are a possibility. Although atmospheric absorption increases as one descends into the millimeter wave region, there are well defined absorption minima at 35, 94, 220, and 325 GHz. As compared with conventional microwave radars, radars operating at millimeter wavelengths would have the advantage of narrow beam width, large bandwidth, and small antenna size. Narrow beam width, for example, would have important applications to low elevation angle tracking. Large bandwidth enhances resistance to electronic countermeasures, and permits high range resolution. Millimeter waves are less affected by fog, clouds, rain, or smoke, than are optical or infrared waves. Thus, millimeter waves have some potential advantages in the area of imaging or semi-imaging radars. There are, of course, some difficulties with millimeter wave radars. The typical CRM uses superconducting magnets to achieve the high magnetic field necessary for operation at the first harmonic. Superconducting systems are not especially attractive for practical radar applications. This problem can be alleviated somewhat by closed loop cryogenic systems. If efficient CRM sources can be developed at higher harmonics, then permanent magnets can be utilized, thereby overcoming the cryogenic problems. The FEL, even at millimeter wavelengths, are presently too large to be practical for most radar applications. Also the high voltages at which they operate will

argue against their utility in radar applications. A practical problem in the development of millimeter wave radars has been the lack of millimeter wave components. The field of millimeter wave components, however, is developing quite rapidly, and this should not be an impediment to the deployment of millimeter wave radars in the future. The use of millimeter waves for surveillance purposes is hampered by the small radar antenna size. This can be compensated to some extent by the very high power which these new millimeter sources promise. The actual radar applications remain to be demonstrated. Nevertheless, it is clear that the FEL and the CRM may open up an important part of the spectrum which previously has been unavailable for radar applications.

The FEL and the CRM are new sources which to date have been the subject of research programs. So far, the results of this research has indicated that these sources represent an important addition to the arsenal of electromagnetic devices. The successful accomplishment of even a few of the applications discussed above will be significant. Like all significant advances in technology, it is very likely that the ultimate and most important applications have yet to be identified.

Acknowledgments

We gratefully acknowledge assistance from Cha-Mei Tang in preparing this article.

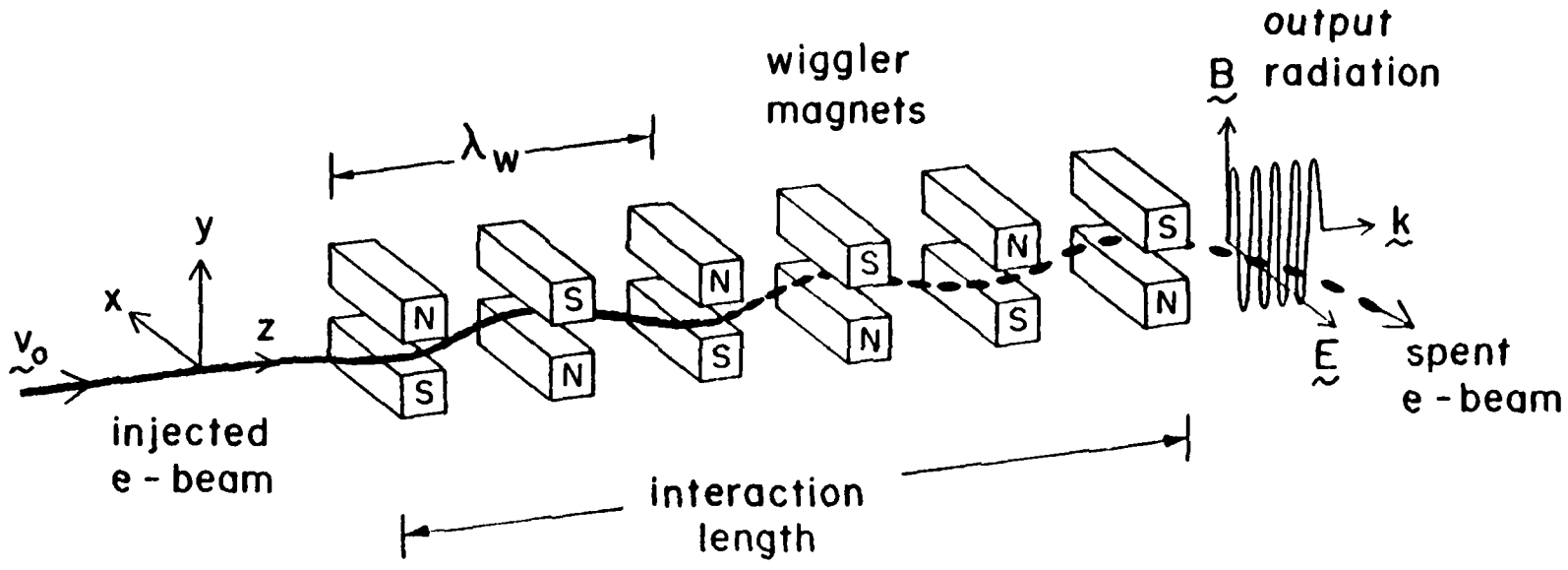

Fig. (1) Basic components of a FEL. The pump field is a magnetic wiggler produced by a periodic arrangement of magnets in which the electrons undergo transverse oscillations. This small velocity component (wiggle velocity) in the direction of the radiation electric field can cause the electrons to lose energy and in turn amplify the radiation field.

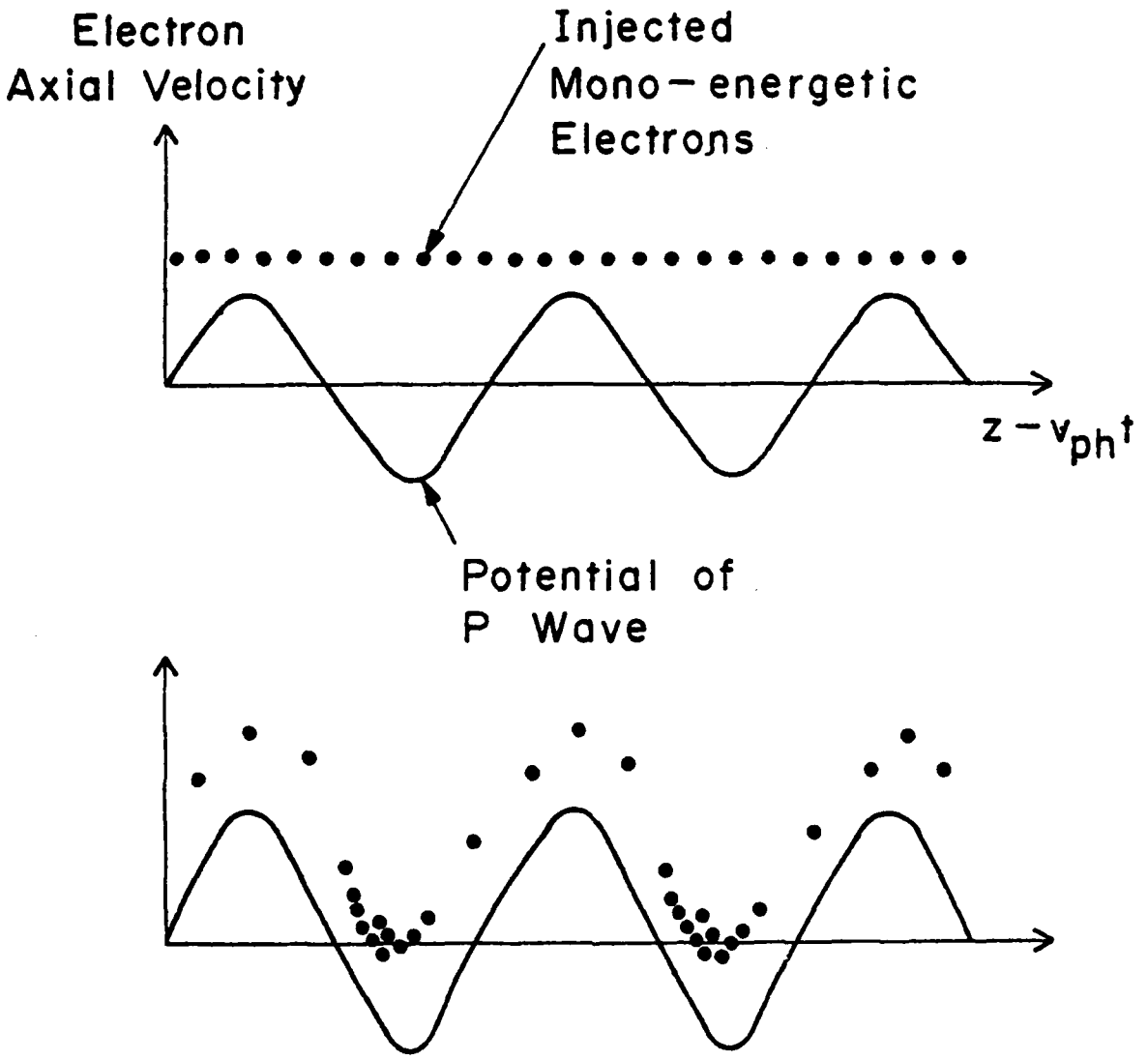

Fig. (2) Interaction of a mono-energetic beam of electrons with the ponderomotive wave potential as seen in the beam frame. a) Initially the injected electrons have an axial velocity slightly greater than the wave phase velocity. The wave potential is shown for reference purposes. b) Later in the interaction electrons, depending on their phase, will either lose or gain energy from the wave. Those that are decelerated fall into the wave potential and become bunched. Since more electrons lose energy than gain energy the radiation field is enhanced.

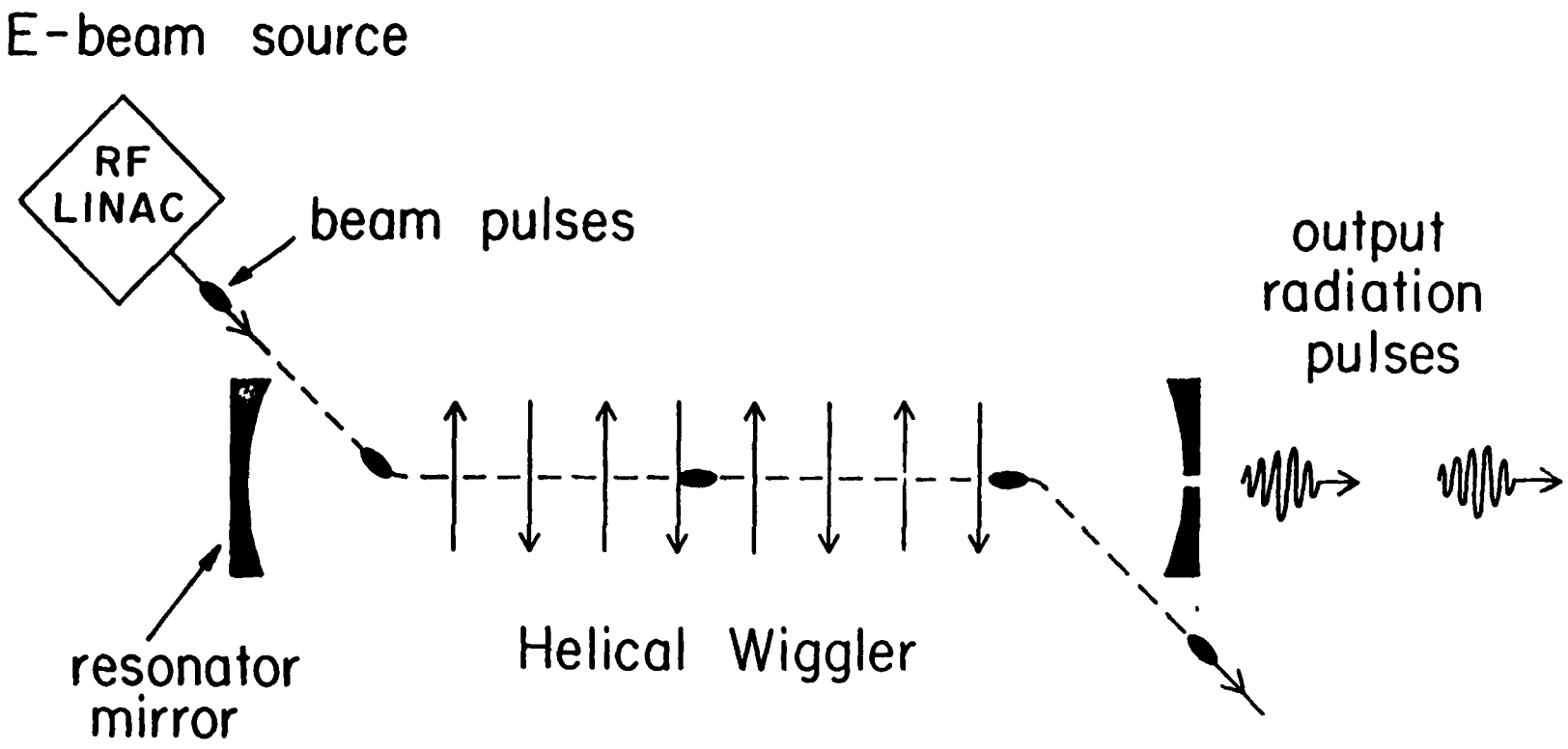

Fig (3) Schematic of FEL oscillator. The pulsed electron beam source is an RF linac. The micro beam pulse spacing and resonator length are such that the reflecting radiation pulses are synchronized with the incoming beam pulses. The mirror on the right is partially transmitting so that a small fraction of the transiting radiation pulses within the resonator (not shown) can escape.

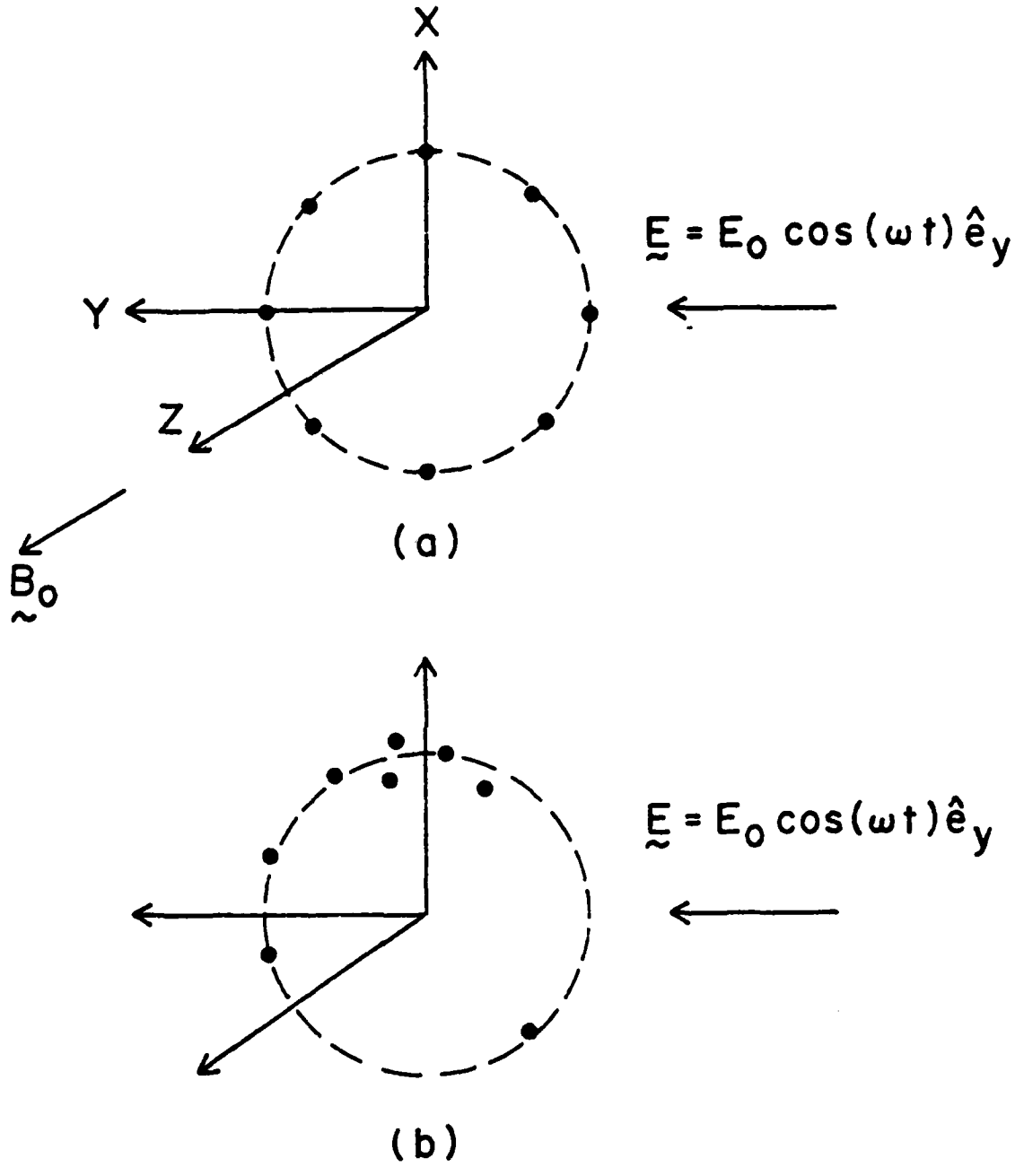

Fig (4) Distribution of gyrating electrons and radiation field demonstrating the ECM mechanism. a) initial electron phase distribution and field polarization b) electron distribution after an integer number of wave periods for $\omega \gtrsim \Omega_R$. Here bunching occurs in phase with the wave producing a decrease in the average electron energy.

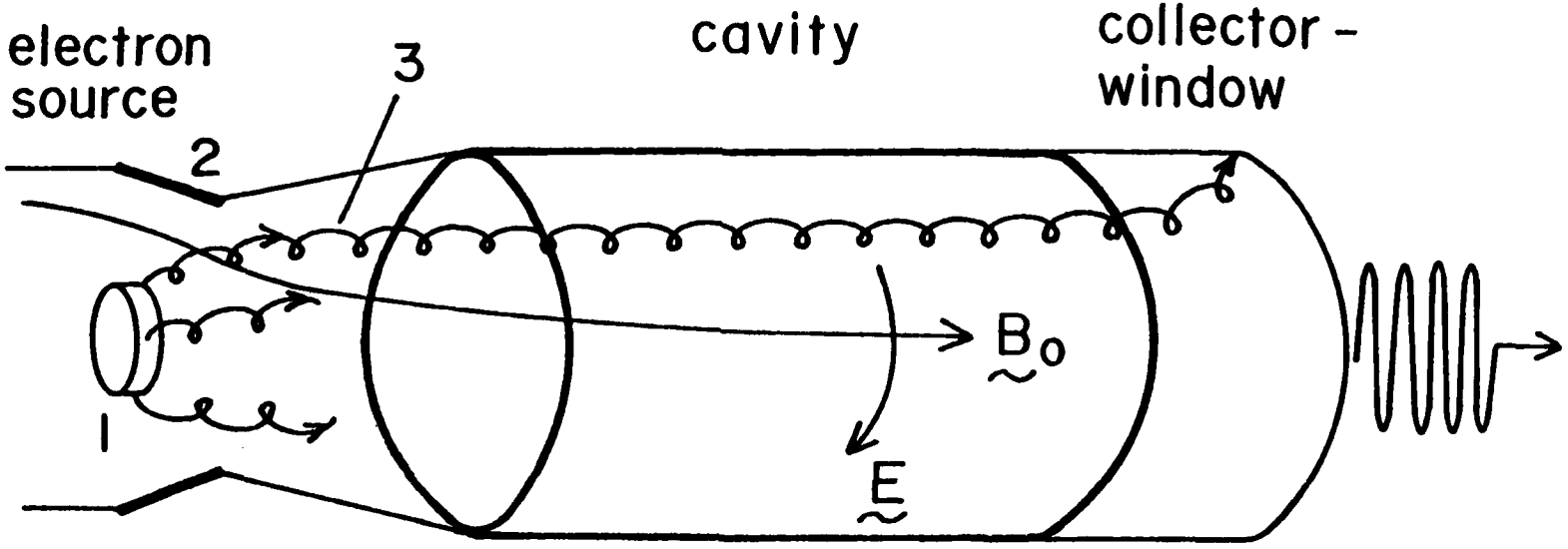

Fig (5) Schematic of an overall CRM oscillator. The electron beam source is a magnetron, i.e., cross field, injection gun, which consist of a cathode (1) and anode (2). The cathode produces an annular electron beam (3) which propagates along and gyrates about the applied magnetic field $\underset{\sim}{B}_o$ into a cavity. The cavity operates in a TE mode near cut-off. The spent electron beam is collected and radiation is emitted through the output window.

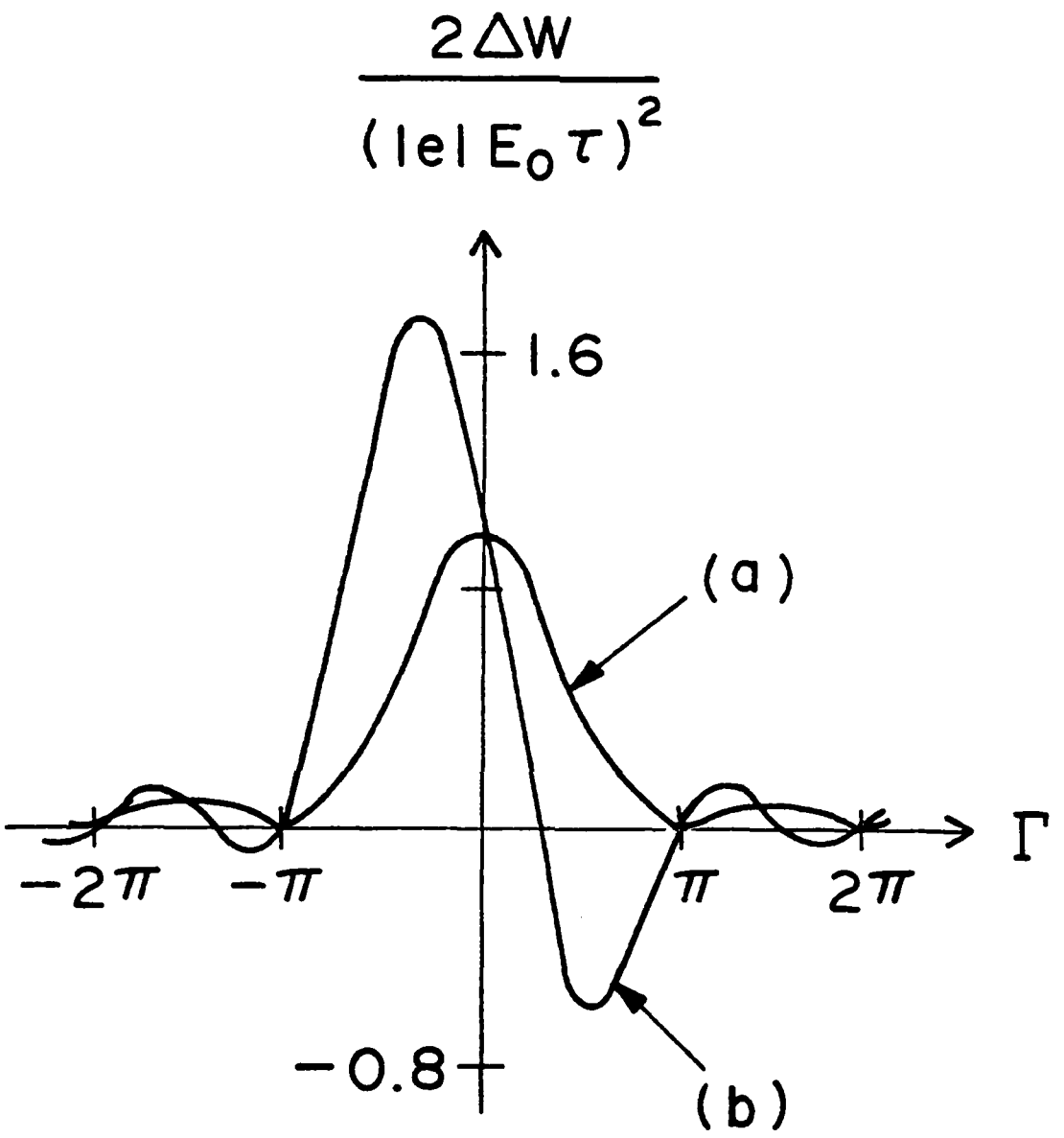

Fig (6) The cyclotron resonance absorption function in the small signal regime is plotted for, a) $\tau(\beta_\perp\Omega_R/2)^2 = 0$ and b) $\tau(\beta_\perp\Omega_R/2)^2 = 4$. Maximum negative absorption, wave amplification, occurs for $\Gamma = \pi/2$.

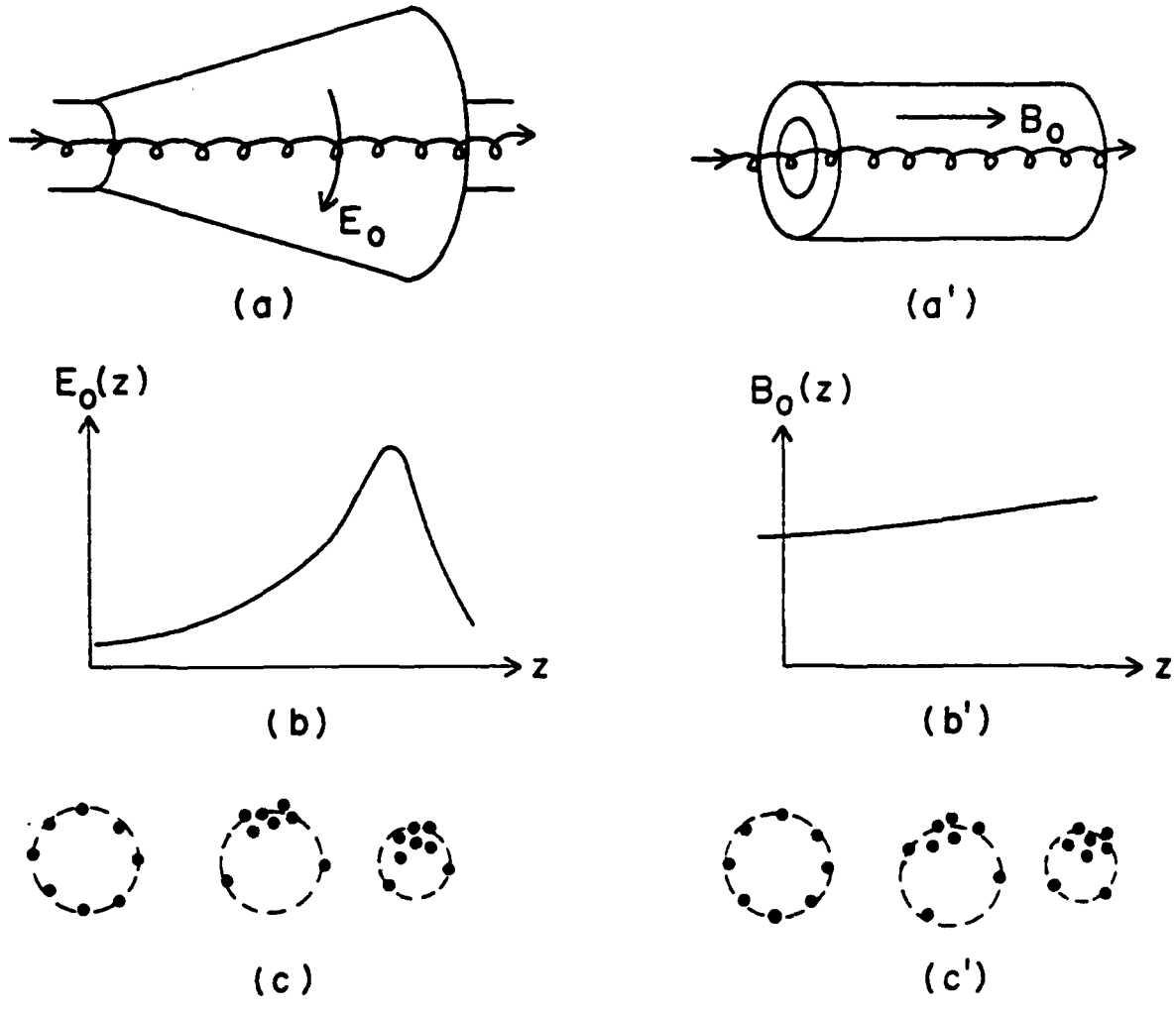

Fig (7) Illustration of the two most commonly employed methods of enhancing efficiency in the CRM oscillator, (a) cavity with longitudinally varying wall radius, (b) longitudinal profile of cavity field (TE mode near cut-off), (c) typical electron phase distribution at various positions within cavity, (a′) constant wall radius cavity, (b′) longitudinal variation in external magnetic field, (c′) same as (c).

References

1. W. B. Colson, Phys. Lett. 64A, 190 (1977).

2. N. M. Kroll and W. A. McMullin, Phys. Rev. A 17, 300 (1978).

3. A. A. Kolomenskii and A. N. Lebedev, Sov. J. Quantum Electron 8, 879 (1978).

4. P. Sprangle, R. A. Smith and V. L. Granatstein, Infrared and Millimeter Waves, Vol. 1, K. J. Button, ed. New York: Academic Press (1979). p. 279.

5a. Free-Electron Generators of Coherent Radiation, Physics of Quantum Electronics, Volume 7, S. F. Jacobs, H. S. Pilloff, M. Sargent III, M. O. Scully and R. Spitzer eds. (Addison-Wesley, 1980).

5b. ibid, volume 8.

5c. ibid, volume 9.

6. R. C. Davidson and W. A. McMullin, Phys. Fluids 26, 840 (1983).

7. H. Freund, Phys. Reveiw A, 27, 1977 (1983).

8. H. H. Fleischmann, Physics Today, Vol. 28, No. 5, May 1975, page 35.

9. D. Keef, Particle Acclerators, 11, 187 (1981).

10. P. Sprangle, C. M. Tang and W. Manheimer, Phys. Review A, 21, 302 (1980).

11. L. R. Elias, W. M. Fairbank, J. M. J. Madey, H. A. Schwettman and T. I. Smith, Phys. Rev. Lett. 36, 717 (1976).

12. Bendor Free Electron Laser Conf., Journal de Physique 44, Collogue C1 (1983).

13. IEEE Journal of Quantum Electronics, Special Issue on Free-Electron Lasers, Vol. QE-19, (1983).

14. C. Goldstein and W. B. Colson, Int'l. Conf. on Lasers, New Orleans, LA, Dec. 13-17 (1982).

15. C. M. Tang and P. Sprangle, Proc. of the Free Electron Laser Workshop, Orcas Island, WA, June 26 - July 1, 1983.

16. J. Pasour, R. Lucey and C. Roberson, Proc. of the Free Electron Laser Workshop, Orcas Island, WA, June 26 - July 1, 1983.

17. Laser Acceleration of Particles, AIP Conference Proceedings, No 91, Paul J. Channell ed. Los Alamos National Laboratory (1982).

18. P. Sprangle and A. T. Drobot, IEEE Trans. MTT-25, 528 (1977).

19. V. L. Granatstein, M. E. Read and L. R. Barnett, Infrared and Millimeter Waves, Vol 5, Pt. I, K. J. Button, ed., Academic Press, New York (1982). Pg. 267.

20. IEEE Trans. (special issue) MTT-25, No. 6 (1977).

21. P. Sprangle and R. Smith, J. Appl. Phys. 51, 3001 (1980).

22. A. A. Andronov, et al., Infrared Physics: Vol. 18, No. 5/6, pp. 385-393, Dec. 1978.

23. V. A. Flyagin, A. G. Luchinin, and G. S. Nusinovich, Int'l. J. of Infrared and Millimeter Waves, Vol. 3, 765 (1982).

24. Y. Carmel, K. R. Chu, M. Read, A. K. Ganguly, D. Dialetis, R. Seeley, J. S. Levine, and V. L. Granatstein, Phys. Rev. Lett. 50, 112 (1983).

25. L. R. Barnett, Y. Y. Lau, K.R. Chu and V. L. Granatstein, IEEE, Trans. ED-28, 872 (1981).

26. P. Sprangle, J. Vomvoridis and W. Manheimer, Phys. Review A, 23, 3127 (1981).

27. N. A. Ebrahim, Z. Liang and J. L. Hirschfield, Phys. Rev. Lett. 49, 1556 (1982).

28. R. A. Mahaffey, P. Sprangle, J. Golden and C. A. Kapetanakos, Phys. Rev. Lett. 39, 843 (1977).

29. G. Bekefi, T. J. Orzechowski, Phys. Rev. Lett., 37, 379 (1976).

30. The Free Electron Laser, the report of the free electron laser Subcommittee of the Solid State Sciences Committee, National Academy of Sciences, National Academy Press (1982).